Int J Clin Exp Pathol 2015;8(9):9875-9888
www.ijcep.com /ISSN:1936-2625/IJCEP0010961

Original Article

Flk-1^{+}Sca-1^{-} mesenchymal stem cells: functional characteristics in vitro and regenerative capacity in vivo

Yugang Li[1], Enshan Pan[1], Yu Wang[1], Xiaoguang Zhu[1], Anyang Wei[2]

[1]Hospital of Integrated Traditional Chinese Medicine & Western Medicine, Southern Medical University, Guangzhou 510315, China; [2]Department of Urology, Medical Center for Overseas Patients, Nanfang Hospital, Southern Medical University, Guangzhou 510515, China

Received June 1, 2015; Accepted July 21, 2015; Epub September 1, 2015; Published September 15, 2015

Abstract: Objectives: Mesenchymal stem cells (MSCs) represent a powerful tool in regenerative medicine because of their differentiation and migration capacities. We aimed to investigate the possibility of Flk-1^{+}Sca-1^{-} mesenchymal stem cells (Flk-1^{+}Sca-1^{-} MSCs) transplantation to repair erectile function in patients suffering from diabetes mellitus (DM)-associated erectile dysfunction (ED). Methods: In this study, we isolated Flk-1^{+}Sca-1^{-} MSCs from bone marrow (bMSCs). Then, newborn male rats were intraperitoneally injected with 5-ethynyl-2-deoxyuridine for the purpose of tracking endogenous Flk-1^{+}Sca-1^{-} MSCs. Eight weeks later, 8 of these rats were randomly chosen to serve as normal control (N group). The remaining rats were injected intraperitoneally with 60 mg/kg of streptozotocin (STZ) to induce DM. Eight of these rats were randomly chosen to serve as DM control (DM group) while another 8 rats were subject to Flk-1^{+}Sca-1^{-} MSCs treatment (DM+MSC group). All rats were evaluated for erectile function by intracavernous pressure (ICP) measurement. Afterward, their penile tissues were examined by histology. Results: Flk-1^{+}Sca-1^{-} MSCs could differentiate into skeletal muscle cells and endothelial cells *in vivo* and *in vitro*. Engrafted Flk-1^{+}Sca-1^{-} MSCs were shown to home to injured muscle, participate in myofibers repair and could partially reconstitute the sarcolemmal expression of myocardin and ameliorate the level of related specific pathological markers. Conclusion: Flk-1^{+}Sca-1^{-} MSCs could be used in the treatment erectile function in diabetes mellitus associated erectile dysfunction by promoting regeneration of nNOS-positive nerves, endothelium, and smooth muscle in the penis.

Keywords: Flk-1^{+}Sca-1^{-} mesenchymal stem cells (Flk-1^{+}Sca-1^{-} MSCs), diabetes mellitus (DM), erectile dysfunction (ED), myocardin, nNOS

Introduction

Bone marrow-derived mesenchymal stem cells (bMSCs) offer the potential to open a new frontier in medicine [1]. Regenerative medicine aims to replace defective cells under a broad range of conditions associated with damaged cartilage, bone, muscle, tendons and ligaments [2]. Diabetes mellitus (DM) is a major risk factor for the development of erectile dysfunction (ED) [3]. The prevalence of ED is higher in the diabetic male population compared with non-diabetic men [4]. Also, ED in men with diabetes is more severe4, with poor response to phosphodiesterase 5 inhibitors compared with non-diabetic patients [5-7]. Stem cell therapy is one of the strategies for ED treatment currently being investigated.

In a previous study, we isolated an Flk1^{+}Sca-1^{-} mesenchymal stem cell subset from adult bone marrow (bMSCs) and found they had not only the three germ layers of cell differentiation potential [5], but significant immunomodulatory capacity [6, 7]. A large number of studies [8-12] have shown that bone marrow-derived adherent cell has a large capacity for self-renewal while maintaining its multipotency which helped to recover the pathogenesis changes in ED from DM patients. bMSCs exert a potent immunosuppressive effect *in vitro*, and thus may have a therapeutic potential in T cell-dependent pathologies. It has been demonstrated that mouse, non-mouse primate, and mouse bMSCs can inhibit T cell proliferation induced either in a MLR or by non-specific mitogens [13]. This suppression occurs regardless of the MHC of bMSCs, and the stimulator and responder lymphocytes [14]. The immunoregulatory effect of bMSCs appears to be, at least in part, mediated by the production of cytokines such as TGFβ-1

and hepatocyte growth factors, and is independent of the induction of apoptosis [15]. These immunosuppressive properties of bMSCs open attractive possibilities in the fields of organ transplantation and repair therapy [16].

Thus, in this study, we aimed to establish a preclinical mouse model to evaluate the therapeutic potential of bMSCs on the treatment of diabetes mellitus-associated erectile dysfunction. We aimed to detect the functional characteristics of bMSCs and establish whether bMSCs could be used to control erectile dysfunction, a major side effect of DM.

Material and methods

Animals

Female C57BL/6 mice (H-2kb) aged 6-8-weeks-old were purchased from the Animal Center of the Chinese Academy of Medical Sciences (Beijing, China). Male BALB/c mice (H-2k^d) aged 6-8-weeks-old were purchased from the Animal Center of the Medical College of Beijing University (Beijing, China). All animals were bred and maintained under specific pathogen-free conditions. All animal handling and experimental procedures were approved by the Animal Care and Use Committee of Beijing Hospital.

Flk-1$^+$Sca-1$^-$ bMSC preparation

Isolation and culture of bone marrow-derived MSCs were performed as described previously with some modifications [7]. Briefly, mononuclear cells were separated by a Ficoll-Paque gradient centrifugation (specific gravity 1.077 g/mL; Nycomed Pharma AS, Oslo, Norway) and the sorted cells were plated at concentration of 1 cell/well by limiting dilution in a total of 96 × 10 wells coated with fibronectin (Sigma, St Louis, MO) and collagen (Sigma) for each patient. Culture medium was Dulbecco modified Eagle medium and Ham F12 medium (DF12) containing 40% MCDB-201 medium complete with trace elements (MCDB) (Sigma), 2% fetal calf serum (FCS; Gibco Life Technologies, Paisley, United Kingdom), 1 × insulin transferrin selenium (Gibco Life Technologies), 10-9 M dexamethasone (Sigma), 10-4 M ascorbic acid 2-phosphate (Sigma), 20 ng/mL interleukin-6 (Sigma), 10 ng/mL epidermal growth factor (Sigma), 10 ng/mL platelet-derived growth factor BB (Sigma), 50 ng/mL fetal liver tyrosine kinase 3 (Flt-3) ligand (Sigma), 30 ng/mL bone morphogenetic protein-4 (Sigma), 100 U/mL penicillin and 100 μg/mL streptomycin (Gibco Life Technologies) at 37°C and a 5% CO_2 humidified atmosphere. Culture media were changed every 4 to 6 days.

Phenotypic analysis of bMSCs

Cultured bMSCs were harvested and flow cytometry was performed to analyze the phenotype after Sca-1 micromagnetic bead purification. Cells were washed with PBS containing 0.5% BSA, and incubated with mAbs for 30 minutes at 4°C. For intracellular antigen detection, cells were fixed in 2% paraformaldehyde for 15 minutes at 4°C, and then permeabilized with 0.1% saponin (Sigma) for 1 hour at room temperature. mAbs included a FITC-conjugated Sca-1 mAb, PE-conjugated Ter119 mAb, FITC-conjugated CD34 mAb, FITC-conjugated CD45 mAb, FITC-conjugated streptavidin, and biotin-conjugated mouse anti-mouse H-2k^d mAb, FITC-conjugated mouse anti-mouse I-A^d mAb, FITC-conjugated CD29 mAb, FITC-conjugated CD44 mAb, FITC-conjugated CD13 mAb, FITC-conjugated goat anti-rat IgG, and anti-mouse Flk-1 mAb (Rat, IgG). Same species and isotype IgG was used as the negative control (all mAbs were purchased from Becton-Dickinson, San Jose, CA, USA). Analysis was performed on a FACScan (Becton-Dickinson) using CellQuest software. Dead cells were excluded by gating out low forward scatter plus high propidium iodide-retaining cells.

MLR

Mouse splenocytes were prepared and suspended in RPMI 1640 medium supplemented with 10% (v/v) FCS, 2 mM L-glutamine, 0.1 mM nonessential amino acids (Life Technologies, Grand Island, NY, USA), 1 mM sodium pyruvate, 100 U/mL penicillin, 100 μg/mL streptomycin, 1% HEPES buffer, and 10 μM 2-mercaptoethanol. Responder cells from treated or normal C57BL/6 mice (5 × 10^5 splenocytes/well) together with lethally irradiated (30 Gy) stimulator cells from BALB/C mice (5 × 10^5 splenocytes/well) in a total volume of 0.2 mL medium were plated in triplicate at 37°C with 5% CO_2 in 96-well U-bottom culture plates (NUNC, Roskilde, Denmark). Cultures were pulsed with 1 μCi/well [^{3}H]-TdR (Shanghai Nucleus Research

Institute, Shanghai, China) on day 4, and harvested after 18 hours with a Tomtec (Wallac, Gaithersburg, MD, USA) automated harvester. Thymidine uptake was quantified in a liquid scintillation and luminescence counter (Wallac TRILUX). Results were expressed as the stimulation index (cpm of treated mice/cpm of normal mice).

Endothelial differentiation

The culture-expanded clonal cells, $2 \times 10^4/cm^2$, were plated on fibronectin in serum-free expansion medium with 30 ng/mL VEGF (Sigma-Aldrich) and 10 ng/mL bFGF (Gibco), then cultured for 2 weeks. To demonstrate endothelial differentiation, we used immunohisto-chemical, immunogold, and Western-blot methods. For immunohistochemical study, we used the labeled streptavidin-biotin-immunoperoxidase system (Dako, Carpinteria, Calif) to visualize proteins. Cells were fixed with 4% paraformaldehyde at 20°C, and endogenous peroxidase activity was quenched with 3% peroxide for 10 minutes. Slides were incubated sequentially with rabbit monoclonal antibody against CD31 and mouse monoclonal antibody against vWF (1:150) for 30 minutes, followed by biotin-labeled anti-rabbit IgG or anti-mouse IgG antibody and peroxidase-conjugated streptavidin, and then visualized with the use of diaminobenzidine staining (Sigma-Aldrich). For immunogold labeling, we fixed cells with 2% glutaraldehyde for 5 minutes, washed them with PBS and incubated them in 0.05 mol/L NH4Cl for 15 minutes. After being thoroughly washed with PBS, the cells were exposed to mouse monoclonal antibody against vWF at a 1:100 dilution overnight at 4°C. Next we washed the cells with PBS and exposed them to biotinylated anti-mouse IgG (Amersham, Piscataway, NJ) and streptavidin-gold (Biocell Laboratories, Rancho Doninguez, Calif). Finally we processed the cells for electron microscopy. For Western blotting, we prepared protein extracts from logarithmically growing cells (before and after differentiation) by subjecting them to lysis in buffer (25 mmol/L Tris-HCl, pH 7.4; 0.15 mol/L NaCl, 1% Nonidet P-40, 1 mmol/L EDTA, and 2 mmol/L EGTA). Next the protein lysates were separated on a sodium dodecyl sulfate 7.5% polyacrylamide gel (Bio-Rad, Hercules, Calif) and transferred onto nitrocellulose membrane. After blocking, blots were incubated with mouse monoclonal antibodies against vWF and -actin at a dilution of 1:100 in the blocking solution for 1 hour at room temperature. The blots were washed and incubated with a sheep anti-mouse horseradish peroxidase-conjugated IgG (E. I. du Pont de Nemours, Mass) at a dilution of 1:5000 for 1 hour. We performed immunodetection using the enhanced-chemiluminescence method (Amersham) in accordance with the manufacturer's instructions.

Western blot analysis

SDS-PAGE was performed as described for zymography with the modification, that the gel was polymerized on Net-Fix for PAG (Serva, Heidelberg, Germany) in the absence of gelatin. 3-fold for MMP-9 detection by the use of microsep ultrafiltration devices (Pall Filtron, Dreireich, Germany). Samples (40 ml) were mixed with loading buffer and separated either under reducing conditions in the presence of DL-DTT with prior boiling or under nonreducing conditions without boiling. After electrophoresis, proteins were transferred to polyvinyl difluoride membranes (Pall Filtron) using a semidry blotting apparatus (Pharmacia) and probed with mouse monoclonal antibodies to s-ICAM-1 (0.4 mg/ml) or MMP-9 (0.2 mg/ml), followed by incubation with peroxidase-labeled secondary antibodies (all antibodies were purchased from Amersham, Braunschweig, Germany). Detection was performed by the use of an chemiluminescence system (Amersham) according to the manufacturer's instructions.

Flow cytometry

Cells were collected by centrifugation and washed with cold PBS and supernatant were depleted with litter fluid left, then fixed with -20°C preserved 70% alcohol overnight and then washed 3 times with phosphoric acid. When dissolved with 0.5 mg/ml RNase A for 30 minutes, they were dyed with 65 μg/ml PI for 1 hour. Analysis was performed in a FACS flow cytometer analyzer (BD Biosciences). Values are given as percentages of positive cells and relative intensity of fluorescence, which is an indication of the level of expression.

Statistics

Statistical analysis was performed with SPSS 10.0 software. The paired-sample t-test was used to test the probability of significant differences between samples. Statistical significance was defined as $P < 0.05$.

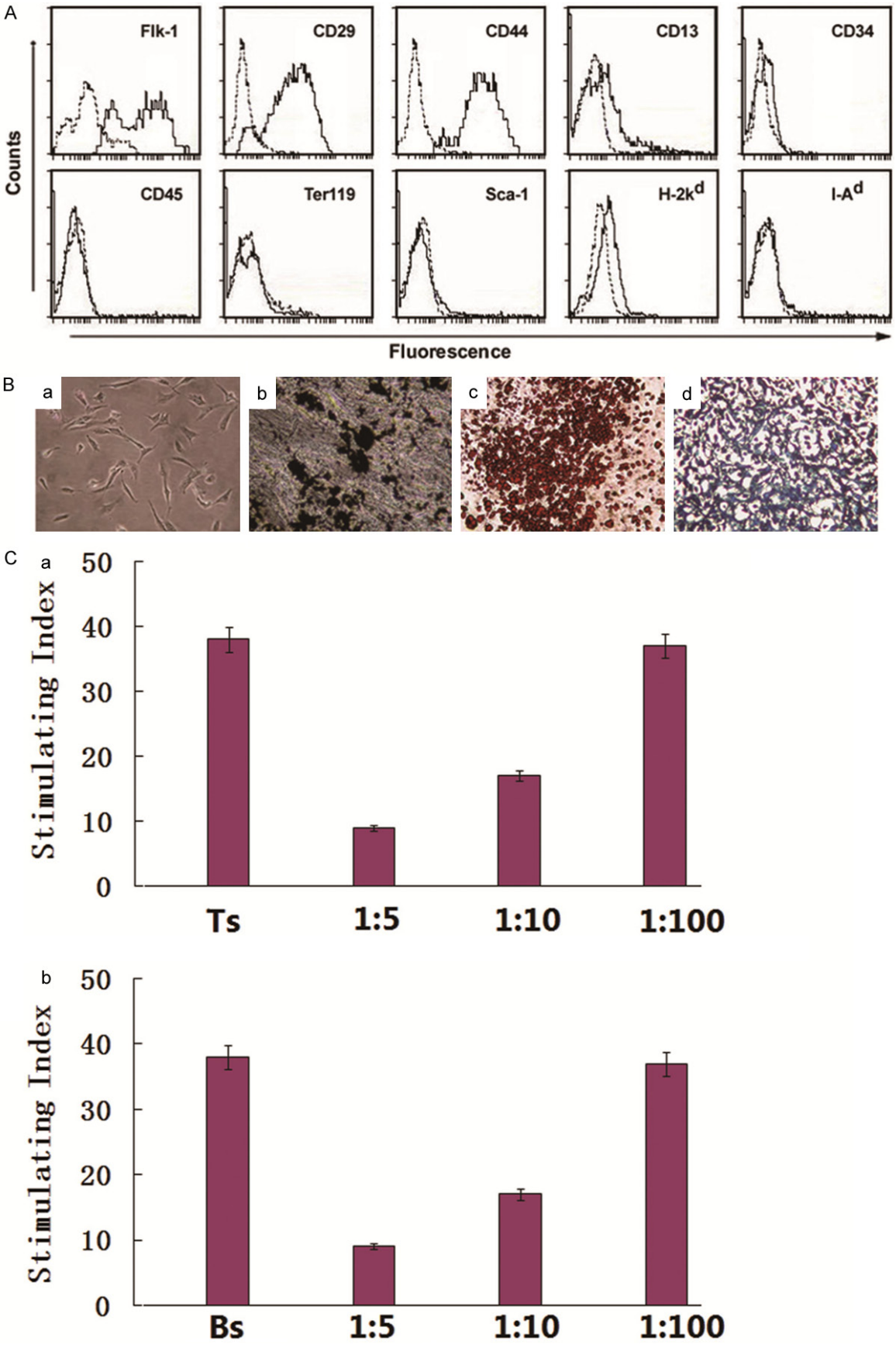
A
Flk-1
CD29
CD44
CD13
CD34
CD45
Ter119
Sca-1
H-2kd
I-Ad
Counts
Fluorescence
B
a
b
c
d
C
a
Stimulating Index
50
40
30
20
10
0
Ts
1:5
1:10
1:100
b
Stimulating Index
50
40
30
20
10
0
Bs
1:5
1:10
1:100

Figure 1. Phenotypic characteristics, morphology and multi-lineage differentiation of mouse Flk-1+ bMSCs. A. Phenotypic analysis of bMSCs showed they were all persistently negative for CD34 and CD31 but positive for Flk1, CD29, CD44 and CD105. B-a. bMSC morphology (magnification, × 100). B-b. Osteogenic differentiation (von-Kossa staining; magnification, × 100). B-c. Adipogenic differentiation (Oil Red-O staining; magnification, × 100). B-d. Chondrogenic differentiation (lycopene-O staining). C. Effect of bMSCs on T or B cell proliferation. bMSCs and splenocytes from normal C57BL/6 mice (H-2Kb) and normal BALB/c (H-2K^d) mice were co-cultured at different proportions (bMSCs:splenocytes = 1:5, 1:10, and 1:100). The proliferation reactions were significantly inhibited at lower proportions of co-culture in a dose-dependent manner. The inhibitory effect was most obvious at 1:5, and the inhibition rate was 87.4%. At 1:100, no significant inhibition was observed in syngeneic or allogeneic groups.

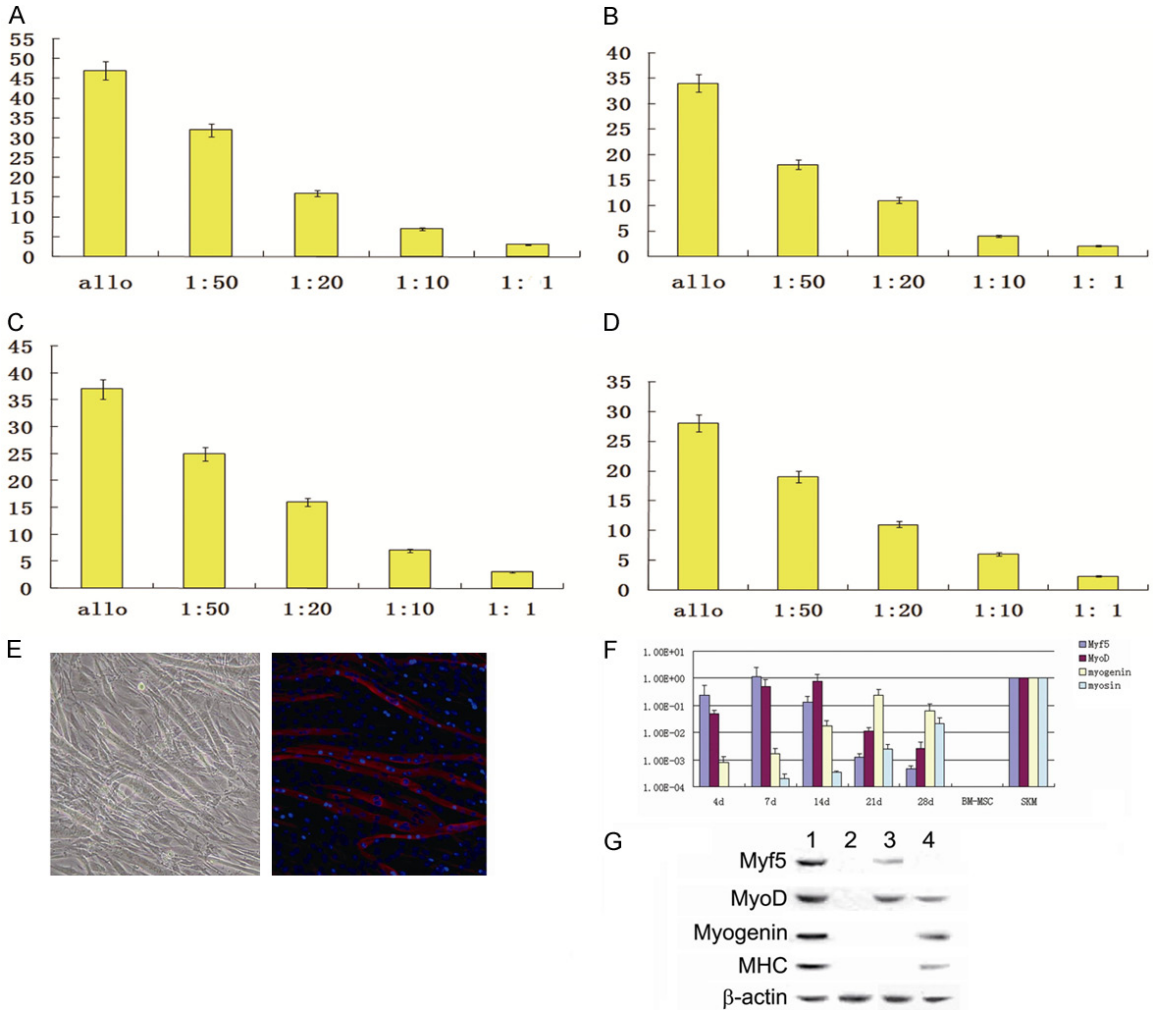

Figure 2. Effects of Flk-1+Sca-1- bMSCs on splenic mononuclear cells proliferation and *in vitro* myogenic differentiation. A. Flk-1+Sca-1- bMSCs inhibited the in vitro proliferation of splenic mononuclear cells. When the ratios of bMSCs to responder cells were 1:50, 1:20, 1:10, and 1:1, the inhibitory rates were 25.12, 56.72, 80.97, and 93.21, respectively ($P < 0.01$). B. When the ratios of bMSCs to allogeneic antigen-stimulated syngeneic splenocytes were 1:50, 1:20, 1:10, and 1:1, the inhibitory rates were 26.43, 57.12, 86.75, and 92.27, respectively ($P < 0.01$). C. bMSCs suppressed the proliferation of allogeneic antigen-stimulated splenocytes in a dose-dependent manner. Co-culture with bMSCs decreased the proliferation rates of splenocytes from ConA-induced syngeneic C57BL/6 and allogeneic BALB/c mice, which positively correlated with the number of splenocytes. At 1:1, the inhibitory effect was most obvious. D. When the ratios of bMSCs to syngeneic splenocytes were 1:50, 1:20, 1:10, and 1:1, the inhibitory rates were 25.72, 45.71, 72.27, and 89.72, respectively ($P < 0.01$). When the ratios of bMSCs to allogeneic splenocytes were 1:50, 1:20, 1:10, and 1:1, the inhibitory rates were 17.21, 45.72, 73.52, and 91.21, respectively ($P < 0.01$). E. Flk-1+Sca-1- bMSCs formed multinucleated myotubes at 4 weeks after myogenic induction. The myogenic differentiation was demonstrated by positive MHC staining (red). Nuclei were stained blue by Hoechst 33342 staining. F. The myogenic gene expression of Flk-1+Sca-1- bMSCs was detected by SQ-real-time RT-PCR analysis with GAPDH as the internal control. Logarithmic scale expression values were normalized to mouse fetal skeletal muscle (ref = 1, n = 5). Values below E-3 were not regarded as expressed. G. Western blot of Myf5, MyoD, Myogenin, and

MHC expression of Flk-1+Sca-1- bMSCs before myogenic induction (lane 2), and 7 d (lane 3), 21 d (lane 4) after myogenic induction. Mouse fetal skeletal muscle biopsy was used as the positive control (lane 1). β-actin was used as the loading control.

Results

Phenotype of Flk-1+Sca-1- bMSCs

bMSCs were generated by culturing bone marrow-derived mononuclear cells that had been depleted of CD45+ and Ter119+ cells by immunomagnetic beads. We found that 91.57% of the harvested cells were positive for Flk-1, a marker of primitive stem cells. Flow cytometric analysis showed that they were positive for CD29 (98.02%), CD44 (98.97%), partly positive for CD13 (18.89%), but negative for CD34, H-2k^d, I-A^d, Sca-1, Ter119, and CD45 (**Figure 1A**).

Multi-lineage differentiation of Flk-1+Sca-1- bMSCs

The results showed that Flk-1+Sca-1- bMSCs persistently displayed a fibroblast-like morphology and could differentiated into bone, fat and cartilage cells, indicating that the isolated cells had stem cell properties (**Figure 1B**).

Inhibition of T and B cell proliferation by Flk-1+Sca-1- bMSCs

To study the effects of Flk-1+Sca-1- bMSCs on T and B cell proliferation, we conducted a ConA-stimulated T or B cell proliferation reaction. bMSCs and splenocytes from normal C57BL/6 mice (H-2K^b) and normal BALB/c (H-2K^d) mice were co-cultured at various proportions (bMSCs:splenocytes = 1:5, 1:10, and 1:100). The proliferation reactions were significantly inhibited at lower proportions of co-cultured cells in a dose-dependent manner. The inhibitory effect was most obvious at 1:5, and the inhibition rate was 87.4%. At 1:100, no significant inhibition was observed in syngeneic or allogeneic groups as shown in **Figure 1C**. These results indicated that the inhibitive effects of bMSCs on T and B cell proliferation were not restricted by MHC and were in a dose dependent manner of bMSCs.

Flk-1+Sca-1- bMSCs inhibit the proliferation of splenic mononuclear cells

We used allogeneic mouse splenocytes as the allogeneic antigen stimulus and allogeneic or syngeneic bMSCs and splenocytes as the responders. The results indicated that Flk-1+Sca-1- bMSCs led to a decrease of the proliferative response of allogeneic antigen-stimulated syngeneic splenocytes and the decrease corresponded positively with the number of bMSCs. When the ratios of bMSCs to responder cells were 1:50, 1:20, 1:10, and 1:1, the inhibitory rates were 25.12, 56.72, 80.97, and 93.21, respectively ($P < 0.01$) (**Figure 2A**). Furthermore, Flk-1+Sca-1- bMSCs inhibited the proliferative response of allogeneic antigen-stimulated syngeneic splenocytes accordingly. When the ratios of Flk-1+Sca-1- bMSCs to responder cells were 1:50, 1:20, 1:10, and 1:1, the inhibitory rates were 26.43, 57.12, 86.75, and 92.27, respectively ($P < 0.01$) (**Figure 2B**).

Flk-1+Sca-1- bMSCs suppress the proliferation of allogeneic antigen-stimulated splenocytes in a dose-dependent manner

We used ConA as the antigenic stimulus, and when bMSCs were co-cultured with splenocytes from ConA-induced syngeneic C57BL/6 or allogeneic BALB/c mice, the proliferation rates were decreased in a dose-dependent manner of splenocytes. When bMSCs and splenocytes were co-cultured at a ratio of 1:1, the inhibitory effect was most obvious. When the ratios of bMSCs to syngeneic splenocytes were 1:50, 1:20, 1:10, and 1:1, the inhibitory rates were 25.72, 45.71, 72.27, and 89.72, respectively ($P < 0.01$) (**Figure 2C**). When the ratios of bMSCs to allogeneic splenocytes were 1:50, 1:20, 1:10, and 1:1, the inhibitory rates were 17.21, 45.72, 73.52, and 91.21, respectively ($P < 0.01$) (**Figure 2D**).

Flk-1+Sca-1- bMSCs undergo myogenic differentiation in vitro

Flk-1+Sca-1- bMSCs formed multinucleated myotubes at 4 weeks after myogenic induction. The myogenic differentiation was demonstrated by positive MHC staining (red). Nuclei were stained blue by Hoechst 33342 staining (**Figure 2E**). The myogenic gene expression of Flk-1+Sca-1- bMSCs (**Figure 2F**) was detected by SQ-real-time RT-PCR analysis with GAPDH as the internal control. Logarithmic scale expression values were normalized to mouse fetal skeletal muscle (ref = 1, n = 5). Values below E-3 were not regarded as expressed. Furthermore, Western blot of Myf5, MyoD, Myogenin,

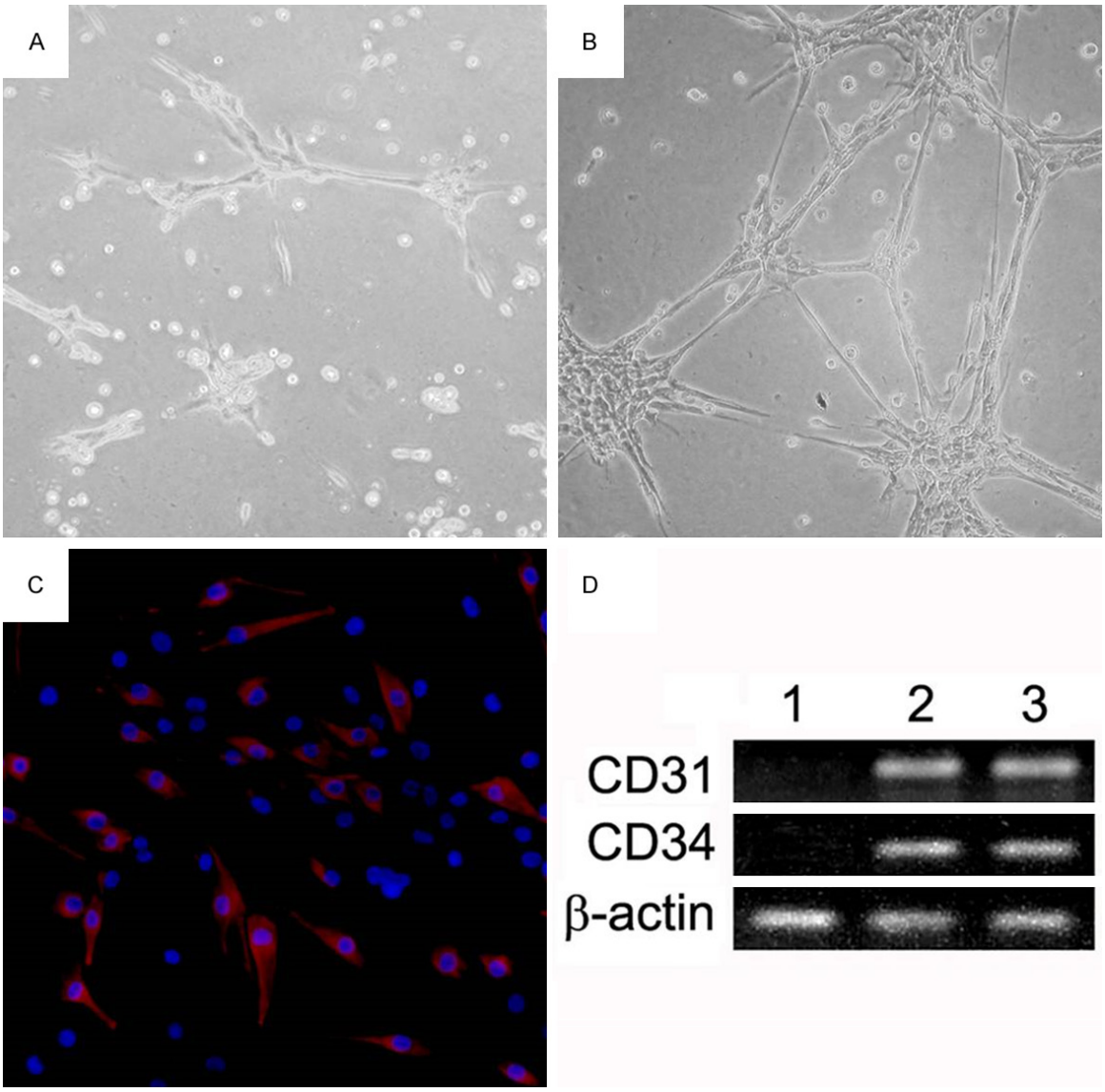

Figure 3. Flk-1+Sca-1- bMSCs undergo endothelial differentiation *in vitro*. A, B. The cell morphology of Flk-1+Sca-1- bMSCs at 12 h (A, × 200) and 48 h (B, × 100) after endothelial induction. C. Immunofluorence: endothelial differentiation of Flk-1+Sca-1- bMSCs was demonstrated by vWF (red) staining (× 200). The nuclei were revealed by Hoechst 33342 staining (blue). D. RT-PCR analysis of mRNA for endothelial markers of Flk-1+Sca-1- bMSCs before induction (lane 1) and 48 h after induction (lane 2). EOMA was used as a positive control (lane 3). β-actin was used as a loading control.

and MHC expression of Flk-1+Sca-1- bMSCs before myogenic induction (lane 2), and 7 d (lane 3), 21 d (lane 4) after myogenic induction (**Figure 2F**). Mouse fetal skeletal muscle biopsy was used as the positive control (lane 1). β-actin was used as the loading control.

Flk-1+Sca-1- bMSCs undergo endothelial differentiation in vitro

The cell morphology of Flk-1+Sca-1- bMSCs at 12 h (**Figure 3A**, × 200) and 48 h (**Figure 3B**, × 100) after endothelial induction. Immunofluorence: endothelial differentiation of Flk-1+Sca-1- bMSCs was demonstrated by vWF (red) staining (× 200). The nuclei were revealed by Hoechst 33342 staining (blue) as shown by **Figure 3C**. RT-PCR analysis of mRNA for endothelial markers of Flk-1+Sca-1- bMSCs before induction (lane 1) and 48 h after induction (lane 2). EOMA was used as a positive control (lane 3). β-actin was used as a loading control (**Figure 3D**).

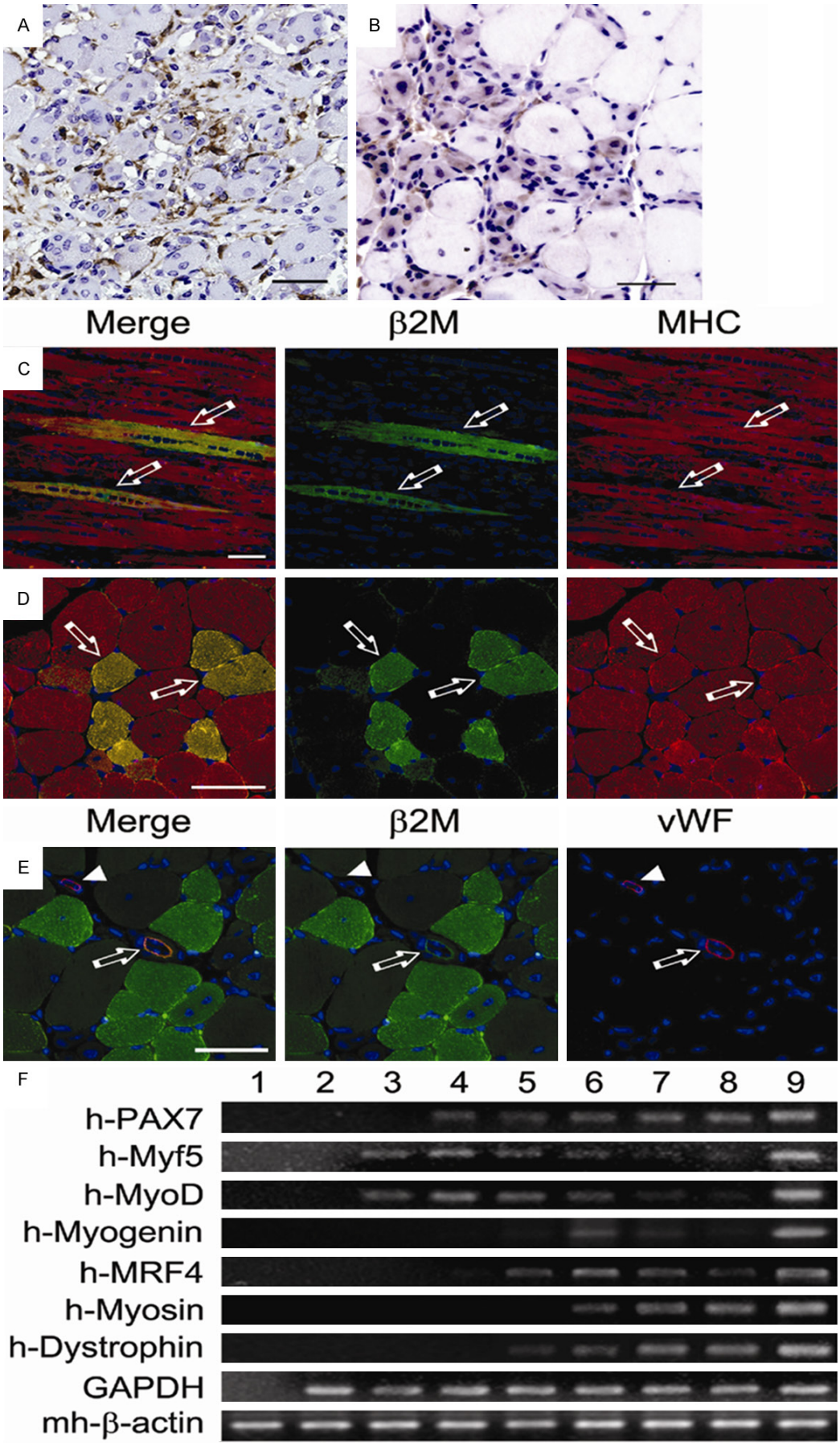
A
B
Merge
β2M
MHC
C
D
Merge
β2M
vWF
E
F
1 2 3 4 5 6 7 8 9
h-PAX7
h-Myf5
h-MyoD
h-Myogenin
h-MRF4
h-Myosin
h-Dystrophin
GAPDH
mh-β-actin

Figure 4. Culture-expanded Flk-1+Sca-1- bMSCs differentiated into myogenic cells and endothelial cells *in vivo*. (A) (B) Immunohistochemistry staining of mouse β2M (brown) in CTX-injured TA muscles at 24 hours (A) and 3 days (B) after transplantation (I.V.). (C) Mouse β2M+ (green), Flk-1+Sca-1- bMSCs-derived MHC+ (red) immature myofibers were characterized by centrally located nuclei at 2 weeks after transplantation (I.V.). (D) Flk-1+Sca-1- bMSCs-derived mature myotube were characterized by peripheral nuclei at 4 weeks after transplantation (I.V.). (E) Double IF staining of mouse β2M (green) and vWF (red) in CTX-injured TA muscles at 4 weeks after transplatation. The nuclei were revealed by Hoechst 33342 staining (blue). The arrow and the arrowhead show donor-derived and host vascular endothelium, respectively. Scale bar, 100 μm. (F) SQ-RT-PCR analysis of Flk-1+Sca-1- bMSCs-injected, regenerative (CTX-treated) TA muscles of C57BL/6 mice at 12 h (lane 3), 1 d (lane 4), 3 d (lane 5), 7 d (lane 6), 14 d (lane 7) and 28 d (lane 8) after injection of Flk-1+Sca-1- bMSCs. TA muscles containing mouse cells were equalized to the expression of mouse GAPHD. TA muscles of CTX-treated mice (with no mouse cells) were used as the control for species specificity of the primers for mouse cDNAs (lane 1). Flk-1+Sca-1- bMSCs and a mouse fetal skeletal muscle biopsy were used as the negative control (lane 2) and the positive control, respectively (lane 9).

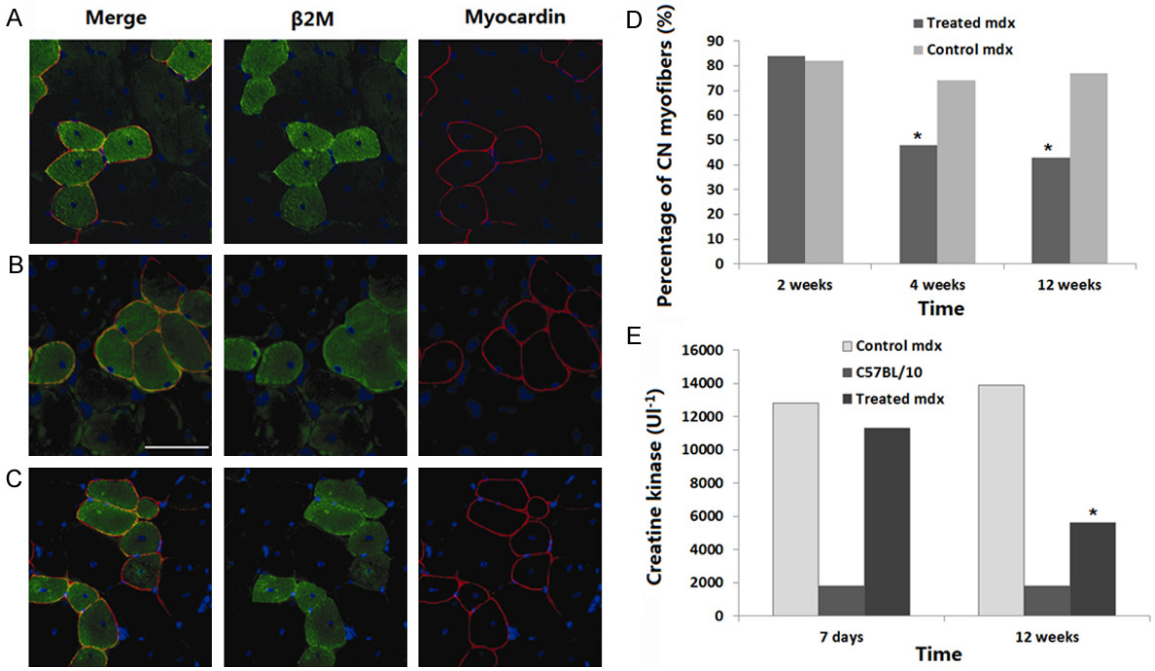

Figure 5. Transplantation of Flk-1+Sca-1- bMSCs restored myocardin expression and partially corrected muscular pathology in mdx mice. (A-C) Double IF staining of mouse β2M (green) and myocardin (red) in CTX-injured TA muscle at 2 weeks (A) and 4 weeks (B) after transplantation, and 2 weeks after the second CTX-treatment (C) (6 weeks after Flk-1+Sca-1- bMSCs transplantation). All nuclei were revealed by Hoechst 33342 staining (blue). Scale bar, 100 μm. (D) The percentage of CN myofibers of TA muscles was not significantly different between the Flk-1+Sca-1- bMSCs-injected group (red) and the control group (blue) at 2 weeks after transplantation (84.5% ± 4.4% vs. 83.2% ± 3.6%, n = 5, $P > 0.8$), but it was significantly lower in the Flk-1+Sca-1- bMSCs-injected group at 4 weeks (48.1% ± 6.2% vs. 72.8% ± 2.3%, n = 5, $P < 0.05$) and 12 weeks (43.3% ± 5.7% vs. 74.2% ± 1.9%, n = 5, $P < 0.05$) after transplantation. (E) At 7 days after Flk-1+Sca-1- bMSCs transplantation, serum CK levels were markedly elevated in the control and the treated groups, compared with normal C57BL/6 mice (12712.8 ± 4091.67 and 11589.6 ± 3455.97 vs. 1735.6 ± 390.79 UI^{-1}, n = 5, $P < 0.005$). After 12 weeks, CK concentrations of the treated mice were significantly decreased, compared with the controls (5321.6 ± 1289.75 vs. 13746.8 ± 5373.75 UI^{-1}, n = 5, $P < 0.005$). C57BL/6 concentrations were 1678.8 ± 352.97 UI^{-1} (red).

Culture-expanded Flk-1+Sca-1- bMSCs differentiated into myogenic cells and endothelial cells in vivo

Immunohistochemistry staining of mouse β2M (brown) in CTX-injured TA muscles at 24 hours (**Figure 4A**) and 3 days (**Figure 4B**) after transplantation. Mouse β2M+ (green), Flk-1+Sca-1- bMSCs-derived MHC+ (red) immature myofibers were characterized by centrally located nuclei at 2 weeks after transplantation (**Figure 4C**). Flk-1+Sca-1- bMSCs-derived mature myotube were characterized by peripheral nuclei at 4 weeks after transplantation (**Figure 4D**). Double

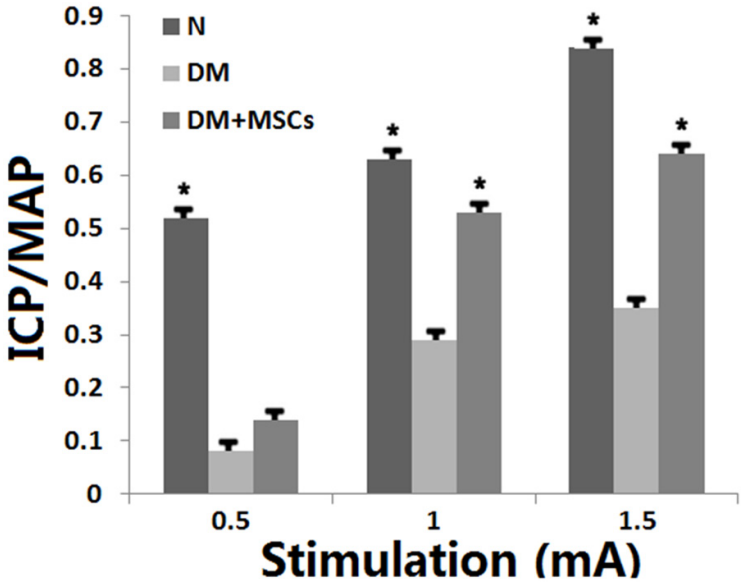

Figure 6. Evaluation of erectile function. Rats in N group (n = 8) were normal control. Rats in DM group (n = 8) were diabetic. Rats in DM+MSC group (n = 8) were diabetic and treated with shockwaves. Their erectile function was evaluated as response in ICP to electrostimulation of cavernous nerves at three different amperages (0.5, 1.0, and 1.5). *Denotes $P < 0.05$ when compared to the DM group.

IF staining of mouse β2M (green) and vWF (red) in CTX-injured TA muscles at 4 weeks after transplantation. The nuclei were revealed by Hoechst 33342 staining (blue). The arrow and the arrowhead show donor-derived and host vascular endothelium, respectively. Scale bar, 100 μm (**Figure 4E**). SQ-RT-PCR analysis of Flk-1+Sca-1- bMSCs -injected, regenerative (CTX-treated, **Figure 4F**) TA muscles of C57BL/6 mice at 12 h (lane 3), 1 d (lane 4), 3 d (lane 5), 7 d (lane 6), 14 d (lane 7) and 28 d (lane 8) after injection of Flk-1+Sca-1- bMSCs. TA muscles containing mouse cells were equalized to the expression of mouse GAPHD. TA muscles of CTX-treated mice (with no mouse cells) were used as the control for species specificity of the primers for mouse cDNAs (lane 1). Flk-1+Sca-1- bMSCs and a mouse fetal skeletal muscle biopsy were used as the negative control (lane 2) and the positive control, respectively (lane 9).

Transplantation of Flk-1+Sca-1- bMSCs restored myocardin expression and partially corrected muscular pathology in mdx mice

Double IF staining of mouse β2M (green) and myocardin (red) in CTX-injured TA muscle at 2 weeks (**Figure 5A**) and 4 weeks (**Figure 5B**) after transplantation, and 2 weeks after the second CTX-treatment (**Figure 5C**). 6 weeks after Flk-1+Sca-1- bMSCs transplantation). All nuclei were revealed by Hoechst 33342 staining (blue). Scale bar, 100 μm. The percentage of CN myofibers of TA muscles was not significantly different between the Flk-1+Sca-1- bMSCs -injected group (red) and the control group (blue) at 2 weeks after transplantation (84.5% ± 4.4% vs. 83.2% ± 3.6%, n = 5, $P > 0.8$), but it was significantly lower in the Flk-1+Sca-1- bMSCs -injected group at 4 weeks (48.1% ± 6.2% vs. 72.8% ± 2.3%, n = 5, $P < 0.05$) and 12 weeks (43.3% ± 5.7% vs. 74.2% ± 1.9%, n = 5, $P < 0.05$) after transplantation (**Figure 5D**). At 7 days after Flk-1+Sca-1- bMSCs transplantation, serum CK levels were markedly elevated in the control and the treated groups, compared with normal C57BL/6 mice (12712.8 ± 4091.67 and 11589.6 ± 3455.97 vs. 1735.6 ± 390.79 UI^{-1}, n = 5, $P < 0.005$). After 12 weeks, CK concentrations of the treated mice were significantly decreased, compared with the controls (5321.6 ± 1289.75 vs. 13746.8 ± 5373.75 UI^{-1}, n = 5, $P < 0.005$). C57BL/6 concentrations were 1678.8 ± 352.97 UI^{-1} (red). (**Figure 5E**).

Flk-1+Sca-1- bMSCs improves erectile function in diabetic rats

Flk-1+Sca-1- bMSCs treatment significantly impaired erectile function as seen in the sharp decline of the ICP/MAP value in DM rats versus normal control (**Figure 6**). Flk-1+Sca-1- bMSCs treatment significantly restored erectile function to levels similar to normal control (at settings of 1.0 and 1.5 mA, **Figure 6**).

Flk-1+Sca-1- bMSCs promotes nerve regeneration

Flk-1+Sca-1- bMSCs treatment caused significant decreases of nNOS-containing nerves in the penis (**Figure 7**). Flk-1+Sca-1- bMSCs treatment partially but significantly restored these nNOS-positive nerves in the sinusoids, around the dorsal arteries, and within the dorsal nerves (**Figure 7**).

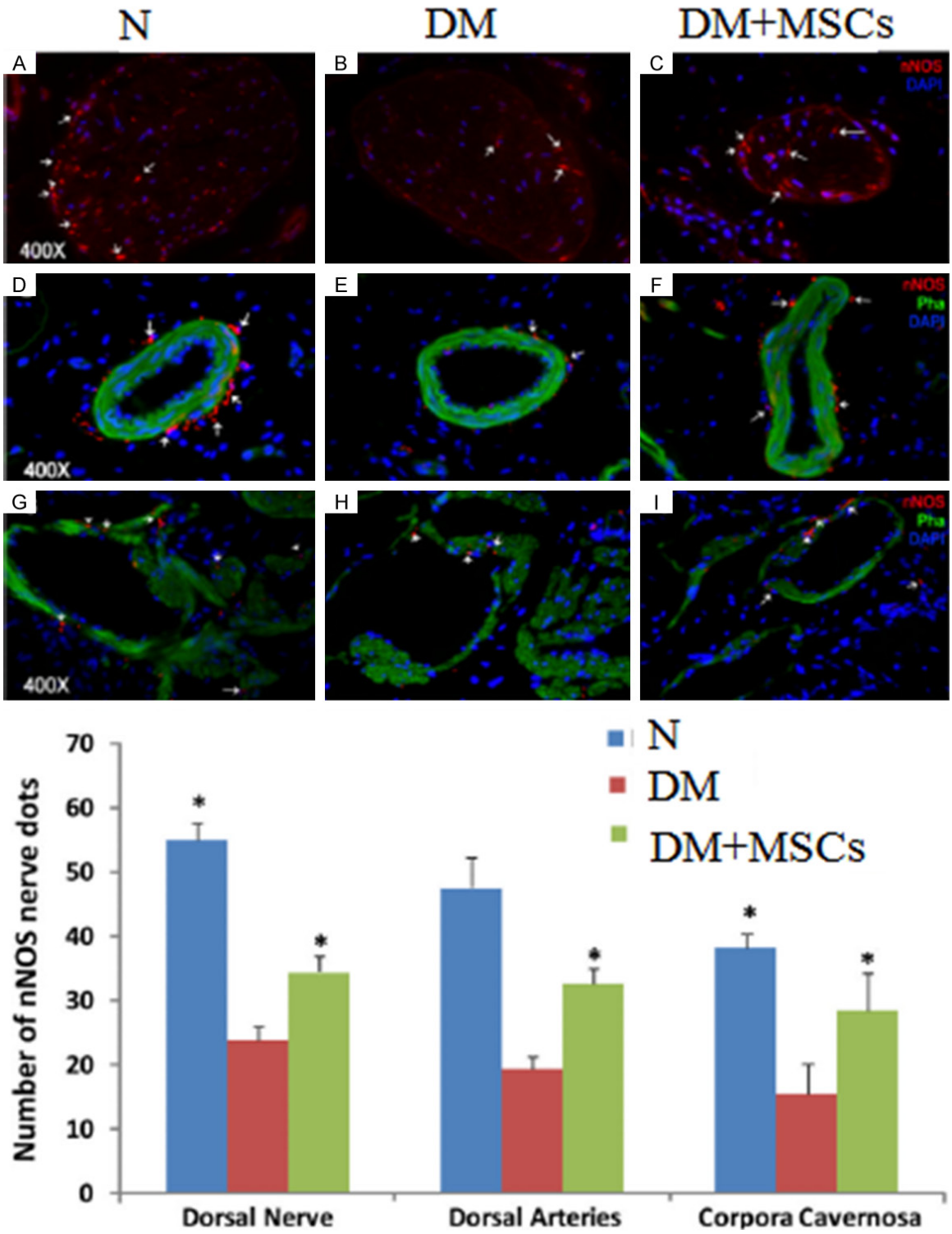

Figure 7. Evaluation of nNOS expression. Rats from penile tissues were examined by IF staining for nNOS expression. The results are shown in the representative histological images with red, green, and blue stains indicating nNOS-positive nerves, smooth muscle, and cell nuclei, respectively. For clarity, the histological images are divided into the dorsal nerves (panels A-C), the dorsal arteries (panels D-F), and the sinusoids (panels G-I). White arrows point at representative nNOS-positive dots. Quantitative data of nNOS expression in these three tissue compartments are shown in the bar chart with the asterisk denoting $P < 0.05$ when compared to the DM group.

Discussion

As with other types of stem cells, MSCs have a high capacity for self-renewal while maintaining their multipotency [17, 18]. Thus, MSCs have an enormous therapeutic potential for tissue repair [19, 20]. MSCs have been shown to be capable of differentiating into multiple cell types including adipocytes, chondrocytes, osteocytes, and cardiomyocytes [21-24].

Despite tremendous advances in the management of ED in the past decade [25], DM-associated ED remains difficult to treat. To overcome this obstacle, one of the proposed therapeutic strategies is stem cell therapy, which has been actively pursued in several clinical and preclinical trials [26]. Another lesser-known strategy is MSC, which has been tested in clinical trials, but in sharp contrast to stem cell therapy, has not been investigated at the preclinical level. Thus, the present study was designed to provide, for the first time, a mechanistic basis for Flk-1+Sca-1- bMSCs' therapeutic effects by using a well-established STZ-induced DM-ED rat model.

STZ-induced diabetic rats have been consistently shown to have poor erectile function [27]. In the present study we further confirmed this observation, and more importantly, we showed that Flk-1+Sca-1- bMSCs significantly improved erectile function in STZ-induced diabetic rats. It has also been known that STZ treatment caused a significant loss of nNOS-positive nerves in rat penis [28], and a recent study also identified a significant reduction of nNOS positive nerves in the penis of diabetic patients [29]. In the present study we showed that, when compared to DM rats, shockwave-treated rats displayed significantly higher numbers of nNOS-positive nerves in different compartments of the erectile tissue, including the dorsal nerves, around the dorsal arteries, and in the corpora cavernosa. This preservation of nNOS-positive nerves thus appears to be an underlying mechanism for Flk-1+Sca-1- bMSCs' therapeutic effects on diabetic patients.

Endothelial injury and dysfunction in cavernous tissue have been consistently identified in diabetic men with ED and in diabetic animal models [30]. Specifically, a reduced cavernous endothelial content is one the most consistent features of STZ-induced diabetic rats [31]. In the present study we found that the endothelial contents in both the cavernous sinusoids and arteries were significantly reduced in STZ-treated rats. More importantly, we also found that Flk-1+Sca-1- bMSCs was able to significantly restore the endothelial contents in both of these two tissue compartments. Thus, protection or regeneration of the endothelium represents another possible underlying mechanism for Flk-1+Sca-1- bMSCs' therapeutic efficacy in diabetic patients. In addition, it has also been shown that diabetic men and animals have reduced cavernous smooth muscle content [22, 26, 27]. In the present study we confirmed this finding in the STZ-treated rats, and more importantly, we showed that Flk-1+Sca-1- bMSCs was able to significantly restore the smooth muscle content.

In all ED-related stem cell studies that have performed histological examination of the erectile tissue, restoration of nNOS-positive nerves, the endothelium, and the smooth muscle has also been consistently observed [32]. In addition, these studies also invariably pointed out that the beneficial tissue effects were likely mediated by stem cell's paracrine capacity [33]. On the other hand, in non-ED fields, the involvement of stem cells in the therapeutic effects of Flk-1+Sca-1- bMSCs has been observed in two instances. In one study of a rat model of bone defects, Flk-1+Sca-1- bMSCs was found to result in the recruitment of MSCs and increased expression of TGF-β and VEGF in the defect tissues [34-37]. In another study of a rat model of chronic hind limb ischemia, Flk-1+Sca-1- bMSCs was also found to enhance recruitment of endothelial progenitor cells in the ischemic tissue [38-40]. Thus, it is conceivable that the tissue effects of Flk-1+Sca-1- bMSCs as observed in the present study might have a stem cell component.

In summary, the present study showed that STZ-induced DM is associated with ED and reduced erectile components (nerves, endothelium, and smooth muscle), and Flk-1+Sca-1- bMSCs was able to partially but significantly restore these function and tissues. Furthermore, we also showed that these beneficial effects of Flk-1+Sca-1- bMSCs were possibly mediated by increased recruitment of MSCs into the erectile tissue.

Acknowledgements

The article was supported by the Dean Foundation of the Hospital of Integrated Traditional Chinese Medicine & Western Medicine, Southern Medical University, China (Grant No.

1201401001) and the Foundation of Science and technology project of Guangdong Province, China (Grant No. 20140211).

Disclosure of conflict of interest

None.

Address correspondence to: Dr. Anyang Wei, Department of Urology, Medical Center for Overseas Patients, Nanfang Hospital, Southern Medical University, Guangzhou 510515, China. E-mail: weianyangvip@163.com

References

[1] He Y, He W, Qin G, Luo J, Xiao M. Transplantation KCNMA1 modified bone marrow-mesenchymal stem cell therapy for diabetes mellitus-induced erectile dysfunction. Andrologia 2014; 46: 479-86.

[2] Kim SJ, Park SH, Sung YC, Kim SW. Effect of mesenchymal stem cells associated to matrixen on the erectile function in the rat model with bilateral cavernous nerve crushing injury. Int Braz J Urol 2012; 38: 833-41.

[3] Qiu X, Lin G, Xin Z, Ferretti L, Zhang H, Lue TF, Lin CS. Effects of low-energy shockwave therapy on the erectile function and tissue of a diabetic rat model. J Sex Med 2013; 10: 738-46.

[4] Kim SJ, Choi SW, Hur KJ, Park SH, Sung YC, Ha YS, Cho HJ, Hong SH, Lee JY, Hwang TK, Kim SW. Synergistic effect of mesenchymal stem cells infected with recombinant adenovirus expressing mouse BDNF on erectile function in a rat model of cavernous nerve injury. Korean J Urol 2012; 53: 726-32.

[5] Sun C, Lin H, Yu W, Li X, Chen Y, Qiu X, Wang R, Dai Y. Neurotrophic effect of bone marrow mesenchymal stem cells for erectile dysfunction in diabetic rats. Int J Androl 2012; 35: 601-7.

[6] Albersen M, Kendirci M, Van der Aa F, Hellstrom WJ, Lue TF, Spees JL. Multipotent stromal cell therapy for cavernous nerve injury-induced erectile dysfunction. J Sex Med 2012; 9: 385-403.

[7] Qiu X, Sun C, Yu W, Lin H, Sun Z, Chen Y, Wang R, Dai Y. Combined strategy of mesenchymal stem cell injection with vascular endothelial growth factor gene therapy for the treatment of diabetes-associated erectile dysfunction. J Androl 2012; 33: 37-44.

[8] Qiu X, Lin H, Wang Y, Yu W, Chen Y, Wang R, Dai Y. Intracavernous transplantation of bone marrow-derived mesenchymal stem cells restores erectile function of streptozocin-induced diabetic rats. J Sex Med 2011; 8: 427-36.

[9] Shen HJ, Zhu GY. Advance of neurogenic erectile dysfunction therapy by stem cells. Fa Yi Xue Za Zhi 2010; 26: 206-9.

[10] Abdel Aziz MT, El-Haggar S, Mostafa T, Atta H, Fouad H, Mahfouz S, Rashed L, Sabry D, Senbel A, Ali GA. Effect of mesenchymal stem cell penile transplantation on erectile signaling of aged rats. Andrologia 2010; 42: 187-92.

[11] Song YS, Lee HJ, Park IH, Kim WK, Ku JH, Kim SU. Potential differentiation of human mesenchymal stem cell transplanted in rat corpus cavernosum toward endothelial or smooth muscle cells. Int J Impot Res 2007; 19: 378-85.

[12] Bivalacqua TJ, Deng W, Kendirci M, Usta MF, Robinson C, Taylor BK, Murthy SN, Champion HC, Hellstrom WJ, Kadowitz PJ. Mesenchymal stem cells alone or ex vivo gene modified with endothelial nitric oxide synthase reverse age-associated erectile dysfunction. Am J Physiol Heart Circ Physiol 2007; 292: H1278-90.

[13] Tadokoro M, Matsushima A, Kotobuki N, Hirose M, Kimura Y, Tabata Y, Hattori K, Ohgushi H. Bone morphogenetic protein-2 in biodegradable gelatin and β-tricalcium phosphate sponges enhances the in vivo bone-forming capability of bone marrow mesenchymal stem cells. J Tissue Eng Regen Med 2012; 6: 253-60.

[14] Park JC, Kim JM, Jung IH, Kim JC, Choi SH, Cho KS, Kim CS. Isolation and characterization of human periodontal ligament (PDL) stem cells (PDLSCs) from the inflamed PDL tissue: in vitro and in vivo evaluations. J Clin Periodontol 2011; 38: 721-31.

[15] Seeberger KL, Eshpeter A, Korbutt GS. Isolation and culture of human multipotent stromal cells from the pancreas. Methods Mol Biol 2011; 698: 123-40.

[16] Sato T, Iso Y, Uyama T, Kawachi K, Wakabayashi K, Omori Y, Soda T, Shoji M, Koba S, Yokoyama S, Fukuda N, Saito S, Katagiri T, Kobayashi Y, Takeyama Y, Umezawa A, Suzuki H. Coronary vein infusion of multipotent stromal cells from bone marrow preserves cardiac function in swine ischemic cardiomyopathy via enhanced neovascularization. Lab Invest 2011; 91: 553-64.

[17] Yu YS, Shen ZY, Ye WX, Huang HY, Hua F, Chen YH, Chen K, Lao WJ, Tao L. AKT-modified autologous intracoronary mesenchymal stem cells prevent remodeling and repair in swine infarcted myocardium. Chin Med J (Engl) 2010; 123: 1702-8.

[18] Macias MI, Grande J, Moreno A, Domínguez I, Bornstein R, Flores AI. Isolation and characterization of true mesenchymal stem cells derived from human term decidua capable of multilineage differentiation into all 3 embryonic layers. Am J Obstet Gynecol 2010; 203: 495.e9-495.e23.

[19] Simmons PJ, Torok-Storb B. Identification of stromal cell precursors in human bone marrow by a novel monoclonal antibody, STRO-1. Blood 1991; 78: 55-62.

[20] Reyes M, Lund T, Lenvik T, Aguiar D, Koodie L, Verfaillie CM. Purification and ex vivo expansion of postnatal human marrow mesodermal progenitor cells. Blood 2011; 98: 2615-25.
[21] Olmsted-Davis EA, Gugala Z, Camargo F, Gannon FH, Jackson K, Kienstra KA, Shine HD, Lindsey RW, Hirschi KK, Goodell MA, Brenner MK, Davis AR. Primitive adult hematopoietic stem cells can function as osteoblast precursors. Proc Natl Acad Sci U S A 2010; 100: 15877-82.
[22] Sordi V, Malosio ML, Marchesi F, Mercalli A, Melzi R, Giordano T, Belmonte N, Ferrari G, Leone BE, Bertuzzi F, Zerbini G, Allavena P, Bonifacio E, Piemonti L. Bone marrow mesenchymal stem cells express a restricted set of functionally active chemokine receptors capable of promoting migration to pancreatic islets. Blood 2005; 106: 419-27.
[23] Lu X, Beck GR Jr, Gilbert LC, Camalier CE, Bateman NW, Hood BL, Conrads TP, Kern MJ, You S, Chen H, Nanes MS. Identification of the homeobox protein Prx1 (MHox, Prrx-1) as a regulator of osterix expression and mediator of tumor necrosis factor α action in osteoblast differentiation. J Bone Miner Res 2011; 26: 209-19.
[24] Chen XD. Extracellular matrix provides an optimal niche for the maintenance and propagation of mesenchymal stem cells. Birth Defects Res C Embryo Today 2010; 90: 45-54.
[25] Morikawa S, Mabuchi Y, Kubota Y, Nagai Y, Niibe K, Hiratsu E, Suzuki S, Miyauchi-Hara C, Nagoshi N, Sunabori T, Shimmura S, Miyawaki A, Nakagawa T, Suda T, Okano H, Matsuzaki Y. Prospective identification, isolation, and systemic transplantation of multipotent mesenchymal stem cells in murine bone marrow. J Exp Med 2009; 206: 2483-96.
[26] Reinisch A, Strunk D. Isolation and animal serum free expansion of human umbilical cord derived mesenchymal stromal cells (MSCs) and endothelial colony forming progenitor cells (ECFCs). J Vis Exp 2009.
[27] Harraz A, Shindel AW, Lue TF. Emerging gene and stem cell therapies for the treatment of erectile dysfunction. Nat Rev Urol 2010; 7: 143-52.
[28] Bakircioglu ME, Lin CS, Fan P, Sievert KD, Kan YW, Lue TF. The effect of adeno-associated virus mediated brain derived neurotrophic factor in an animal model of neurogenic impotence. J Urol 2001; 165: 2103-9.
[29] Park SH, Doh J, Park SI, Lim JY, Kim SM, Youn JI, Jin HT, Seo SH, Song MY, Sung SY, Kim M, Hwang SJ, Choi JM, Lee SK, Lee HY, Lim CL, Chung YJ, Yang D, Kim HN, Lee ZH, Choi KY, Jeun SS, Sung YC. Branched oligomerization of cell-permeable peptides markedly enhances the transduction efficiency of adenovirus into mesenchymal stem cells. Gene Ther 2010; 17: 1052-61.
[30] Deans RJ, Moseley AB. Mesenchymal stem cells: biology and potential clinical uses. Exp Hematol 2000; 28: 875-84.
[31] Sasaki M, Abe R, Fujita Y, Ando S, Inokuma D, Shimizu H. Mesenchymal stem cells are recruited into wounded skin and contribute to wound repair by transdifferentiation into multiple skin cell type. J Immunol 2008; 180: 2581-7.
[32] Aboody KS, Brown A, Rainov NG, Bower KA, Liu S, Yang W, Small JE, Herrlinger U, Ourednik V, Black PM, Breakefield XO, Snyder EY. Neural stem cells display extensive tropism for pathology in adult brain: evidence from intracranial gliomas. Proc Natl Acad Sci U S A 2000; 97: 12846-51.
[33] Levy YS, Bahat-Stroomza M, Barzilay R, Burshtein A, Bulvik S, Barhum Y, Panet H, Melamed E, Offen D. Regenerative effect of neural-induced human mesenchymal stromal cells in rat models of Parkinson's disease. Cytotherapy 2008; 10: 340-52.
[34] Bella AJ, Lin G, Lin CS, Hickling DR, Morash C, Lue TF. Nerve growth factor modulation of the cavernous nerve response to injury. J Sex Med 2009; 6 Suppl 3: 347-52.
[35] Bella AJ, Lin G, Tantiwongse K, Garcia M, Lin CS, Brant W, Lue TF. Brain-derived neurotrophic factor (BDNF) acts primarily via the JAK/STAT pathway to promote neurite growth in the major pelvic ganglion of the rat: part I. J Sex Med 2006; 3: 815-20.
[36] Lin G, Bella AJ, Lue TF, Lin CS. Brain-derived neurotrophic factor (BDNF) acts primarily via the JAK/STAT pathway to promote neurite growth in the major pelvic ganglion of the rat: part 2. J Sex Med 2006; 3: 821-7.
[37] Bella AJ, Lin G, Garcia MM, Tantiwongse K, Brant WO, Lin CS, Lue TF. Upregulation of penile brain-derived neurotrophic factor (BDNF) and activation of the JAK/STAT signalling pathway in the major pelvic ganglion of the rat after cavernous nerve transection. Eur Urol 2007; 52: 574-80.
[38] Yaghoobi MM, Mowla SJ. Differential gene expression pattern of neurotrophins and their receptors during neuronal differentiation of rat bone marrow stromal cells. Neurosci Lett 2006; 397: 149-54.
[39] Qu R, Li Y, Gao Q, Shen L, Zhang J, Liu Z, Chen X, Chopp M. Neurotrophic and growth factor gene expression profiling of mouse bone marrow stromal cells induced by ischemic brain extracts. Neuropathology 2007; 27: 355-63.
[40] Yaghoobi MM, Mahani MT. NGF and BDNF expression drop off in neurally differentiated bone marrow stromal stem cells. Brain Res 2008; 1203: 26-31.